Electronic Supplementary Material (ESI) for RSC Advances.

Supporting Information *for*

The rationality of using core-shell nanoparticles with embedded internal standards for SERS quantitative analysis based glycerol-assisted 3D hotspots platform

Xiao-An Wang,[a,b], Wei Shen,[a] Binbin Zhou,[a,c] Daoyang Yu,[a] Xianghu Tang,* [a] Jinhuai Liu,*[a,b] Xingjiu Huang[a,b]

[a] Environmental Materials and Pollution Control Laboratory, Institute of Solid State Physics, HFIPS, Chinese Academy of Sciences, Hefei 230031, China.

[b] Institute of Physical Science and Information Technology, Anhui University, Hefei 230601, China.

[c] Department of Mechanical Engineering, City University of Hong Kong, Kowloon, Hong Kong, China.

*X.H.T. (tangxh2011@iim.ac.cn). Fax: (+86)551-65591132.

*J.H.L. (jhliu@iim.ac.cn). Fax: (+86)551-65591142.

Section 1: Hydrophobic treatment of silicon wafers.

Hydrophobic silicon wafers were prepared according to the literatures.[1-3] The silicon wafers were firstly rinsed with ethanol, immersed in aqua regia (hydrochloric acid: nitric acid = 3:1, volume ratio) for 2 h, and placed in the ultrasonic cleaner for 0.5 h. Then, the silicon wafers were immersed into a boiling solution prepared by mixing 30% H_2O_2 and concentrated H_2SO_4 (98%) at a volume ratio of 1:3 for 1 h, and rinsed repeatedly with ultrapure water. After repeating step 2 and drying the silicon wafers, immersed them in 40 mm triethoxy-1H, 1H, 2H, 2H-tridecafluoro-n-octylsilane ethanol solution for 2 h, then cleaned with ultrapure water and dried with nitrogen. Finally, the silicon wafers were dried at 120℃ for 2 h for future use. Typical optical images of an aqueous droplet sitting on the hydrophobic silicon wafer at different states over time can be seen in Fig.S1.

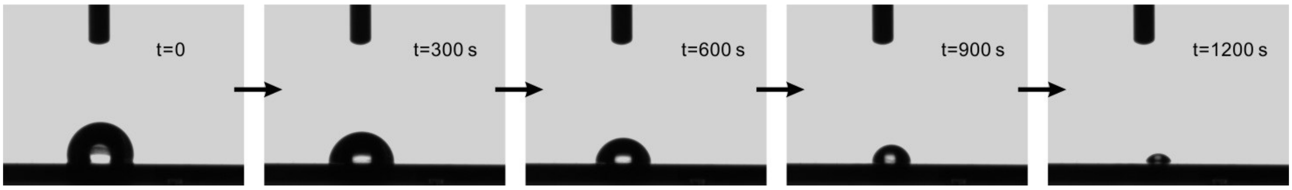

Fig.S1 Optical images of an aqueous droplet sitting on the hydrophobic silicon wafer at different states over time.

Section 2: Size distribution obtained based on the SEM images.

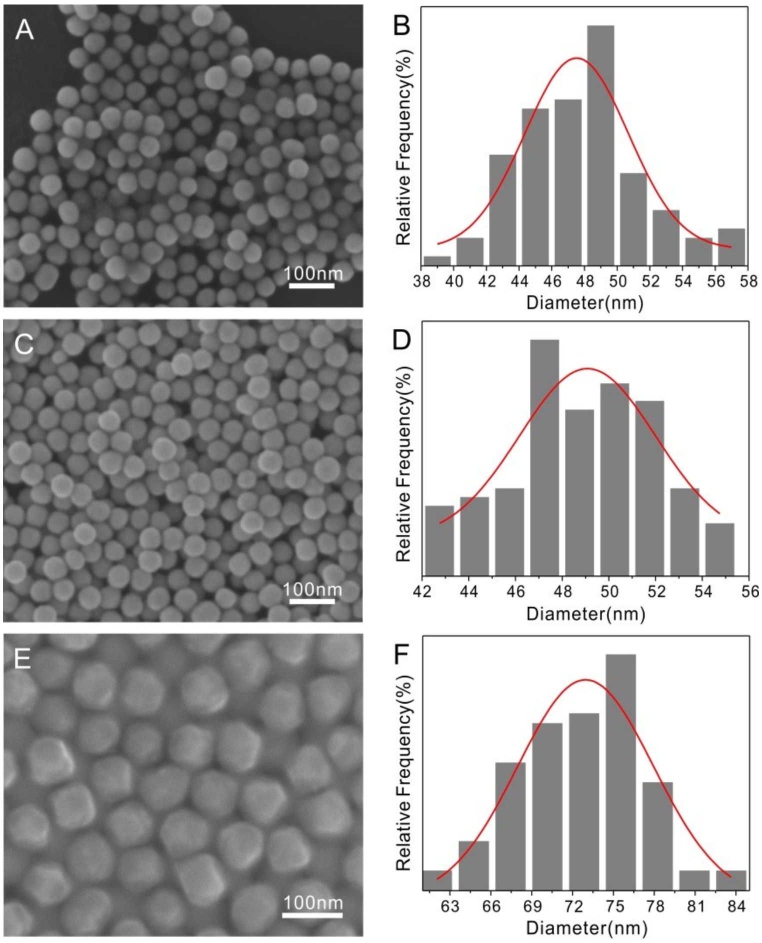

Fig.S2 A and B) SEM and diameter distributions of AuNPs. C and D) SEM and diameter distributions of Au@4-Mpy NPs. E and F) SEM and diameter distributions of Au@4-Mpy@AgNPs.

Section 3: EDS spectrum of Au@4-Mpy@AgNPs.

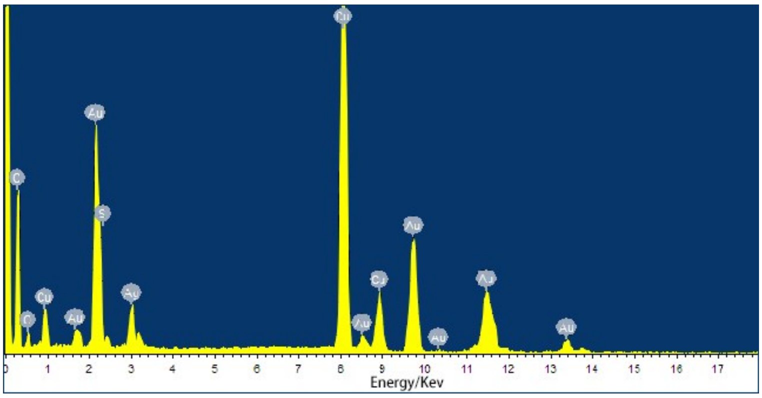

Fig.S3 EDS spectrum of Au@4-Mpy@AgNPs. It is indicated that as-prepared product consists of Au, Ag and S. As a note, the Cu element was detected in the sample originate from copper grids.

Section 4: Optical properties of the AuNPs and Au@4-Mpy NPs.

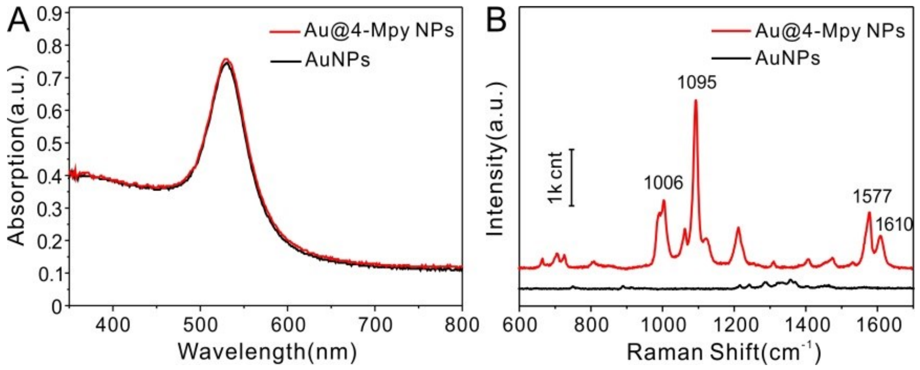

Fig.S4 A) UV−vis absorption spectra of the core of AuNPs (black) and Au@4-Mpy NPs. B) SERS spectra of AuNPs (black) and Au@4-Mpy NPs (red).

Section 5: Absorption spectra of Au@AgNPs and Au@4-Mpy@AgNPs.

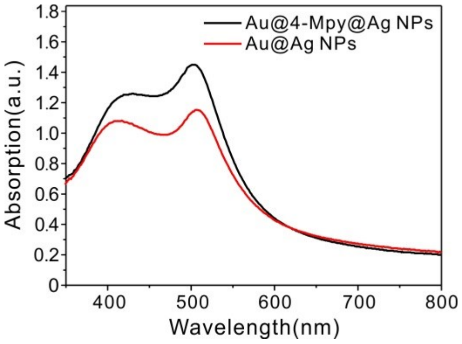

Fig.S5 UV-vis absorption spectra of Au@AgNPs (red) and Au@4-Mpy@AgNPs (black).

Section 6: The zeta potential of AuNPs, Au@4-Mpy NPs and Au@4-Mpy@AgNPs.

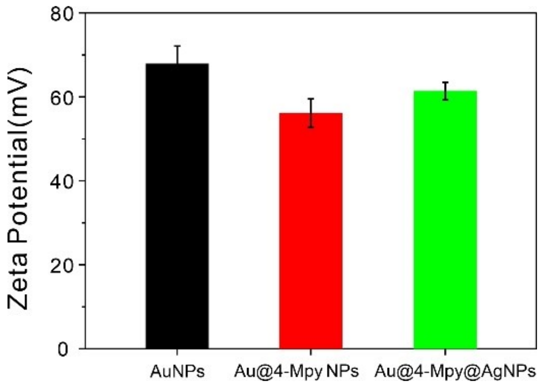

Fig.S6 The zeta potential of AuNPs, Au@4-Mpy NPs and Au@4-Mpy@AgNPs.

Section 7: Calculation of enhancement factor (EF) values for Au@4-Mpy@AgNPs

In order to observe the enhancement intuitively and quantitatively, the SERS EF[4-6] was calculated as follows:

$$\mathrm{EF} = \frac{\mathrm{I_{SERS}}/\mathrm{N_{SERS}}}{\mathrm{I_0}/\mathrm{N_0}}$$

where I_0 and N_0 are the peak intensity and corresponding total number of analyte molecules in the scattering volume (V_{Raman}) for the regular Raman (non-SERS) measurement with 0.05 M 4-Mpy aqueous solution (4-Mpy is slightly soluble in water) on Si wafers, respectively; and I_{SERS} and N_{SERS} are the peak intensity and the average number of embedded molecules in the scattering volume (V_{SERS}) for the SERS experiments, respectively.

The average diameter of the Au core is approximately 48±3 nm. It is reasonable to assume that each particle is spherical. Thus, the sphere surface area of a single particle can be calculated as follows:

$$S_{core}=4\pi R^2$$

where R =24 nm, which is the radius of the Au core.

Table S1 Structural parameters of 4-Mpy.

Atom	Bond Atom	Bond length (Å)	Angle Atom	Angle (°)	Ball & stick model of 4-Mpy linked with Au atom
C(1)					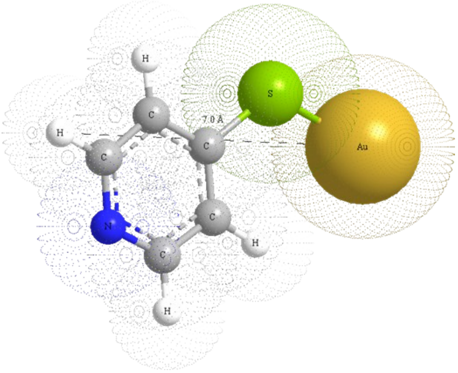
C(2)	C(1)	1.3858			
N(3)	C(2)	1.3509	C(1)	123.7956	
H(10)	C(2)	1.1	C(1)	118.1019	
C(4)	N(3)	1.3509	C(2)	116.6195	
C(5)	C(4)	1.3858	N(3)	123.8024	
H(11)	C(4)	1.1	N(3)	118.0988	
C(6)	C(1)	1.391	C(2)	118.2348	
S(7)	C(6)	1.815	C(1)	120.3421	
H(9)	C(1)	1.1	C(2)	120.8826	
H(12)	C(5)	1.1	C(4)	120.8843	
Au(8)	S(7)	2.36	C(6)	119.9998	

From the structural parameters of 4-Mpy, it can be calculated that each 4-Mpy molecule occupies ~0.49 nm^2 on the surface of Au core. Therefore, the number of molecules loaded per particle can be calculated as follows:

$$N_0=S_{core}/0.49\ nm^2= 4\pi R^2/0.49\ nm^2=1.5\times10^4\ p^{-1}$$

Meanwhile, the concentration of AuNPs was estimated to be ~1 × 10^{10} P/mL. So the apparent concentration of 4-Mpy (loaded molecules) of AuNPs@4-Mpy is:

$$C_{0,\ Mpy/core}=(\ N_0*1\times10^{10}\ P/mL)/N_A=0.25\times\ 10^{-6}\ M$$

Here, N_A represents the Avogadro constant, 6.022×10^{23}.

Furthermore, the calculated value of apparent concentration of 4-Mpy (embedded molecules) of AuNPs@4-Mpy@Ag, $C_{0,\ Mpy/Au@IS@Ag}$, is ~$0.2\times\ 10^{-6}$ M.

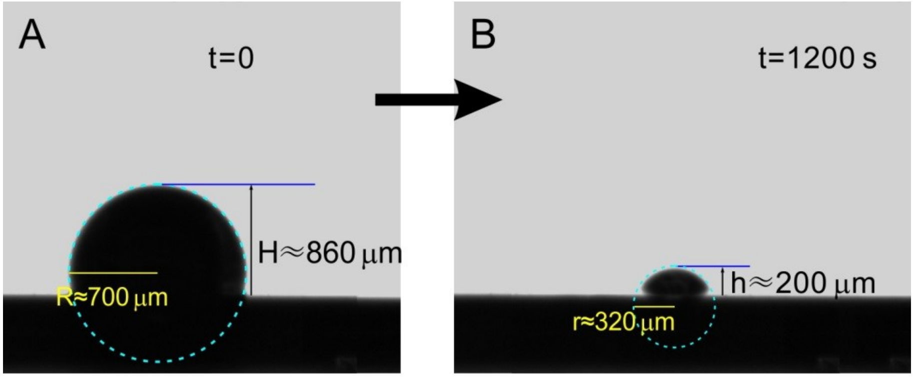

Fig.S7 Measured the height (H, h) of a 1 μL droplet of concentrated AuNP@4-Mpy@Ag sols on the hydrophobic silicon wafer. (A) The initial state of the height (H) was ~860μm. (B) Remaining portion of the evaporating droplet after approximately 1200s, the final state of the height (h) had decreased to ~200 μm.

After 10 mL of AuNP@4-Mpy@Ag sols was concentrated to 20 μL, the apparent concentration of 4-Mpy (embedded molecules) of AuNPs@4-Mpy@Ag, $C_{i,\ Mpy/Au@IS@Ag}$, is ~$1\times\ 10^{-4}$ M.

The initial state of the droplet was about 1μL, and from figure S7, it can be calculated that the final state of the droplet was about: $V_{final}= \pi h^2(r-h/3)=0.032$ μL. Therefore, the apparent concentration of 4-Mpy (embedded molecules) of AuNPs@4-Mpy@Ag, $C_{f,\ Mpy/Au@IS@Ag}$, is ~$3\times\ 10^{-3}$ M.

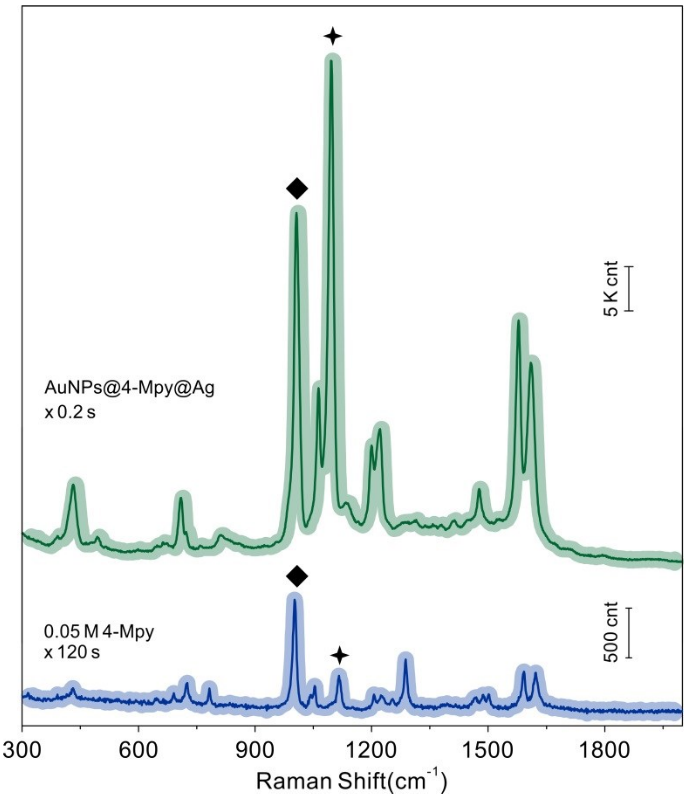

Fig.S8 Raman (0.05 M 4-Mpy aqueous solution) and SERS (embedded molecules of AuNPs@4-Mpy@Ag) of 4-Mpy.

Table S2 Assignments and Raman shifts for Raman and SERS of 4-Mpy. [7-9]

AuNPs@4-Mpy@Ag	0.05 M 4-Mpy aqueous solution	Assignment
SERS / cm^{-1}	Raman / cm^{-1}	
1006	1002	Ring breath
1095	1116	Trigonal ring breath, str C-S

Based on algorithms:

$$EF = \frac{I_{SERS}/N_{SERS}}{I_{Raman}/N_{Raman}} = \frac{I_{SERS}/C_{SERS}V_{SERS}}{I_{Raman}/C_{Raman}V_{Raman}}$$

On account of all of the systems under test are liquid, so the two values of V_{SERS} and V_{Raman} can be considered equal.

Here, Raman and SERS spectra were performed on a LabRAM HR800 confocal microscope Raman system (Horiba Jobin Yvon) using a He–Ne laser operating at 632.8 nm. The laser beam was focused on the sample using a 10× LMPLFLN microscope objective (numerical aperture, NA =

0.25; working distance, WD = 10.6 mm). The laser power was approximately 2 mW. It's worth noting that, under the same laser power condition, the exposure time of the two systems is different. More details of Raman (0.05 M 4-Mpy aqueous solution) and SERS (embedded molecules of AuNPs@4-Mpy@Ag) of 4-Mpy can be seen in Fig.S8.

Based on the intensities of the ring breath vibration modes at 1006 cm^{-1} (SERS spectra: exposure time, 0.2 S; intensity, 43614 cnt) and at 1002 cm^{-1}, (Raman spectra: exposure time, 120 S; intensity, 1250 cnt), the EF was calculated to be 3.5×10^5.

Based on the intensities of the trigonal ring breath vibration modes at 1095 cm^{-1} (SERS spectra: exposure time, 0.2 S; intensity, 60847 cnt) and at 1116 cm^{-1} (Raman spectra: exposure time, 120 S; intensity, 481 cnt), the EF was calculated to be 1.27×10^6, which showing a good SERS activity of the AuNPs@4-Mpy@Ag substrate.

Section 8: SERS spectra of CV.

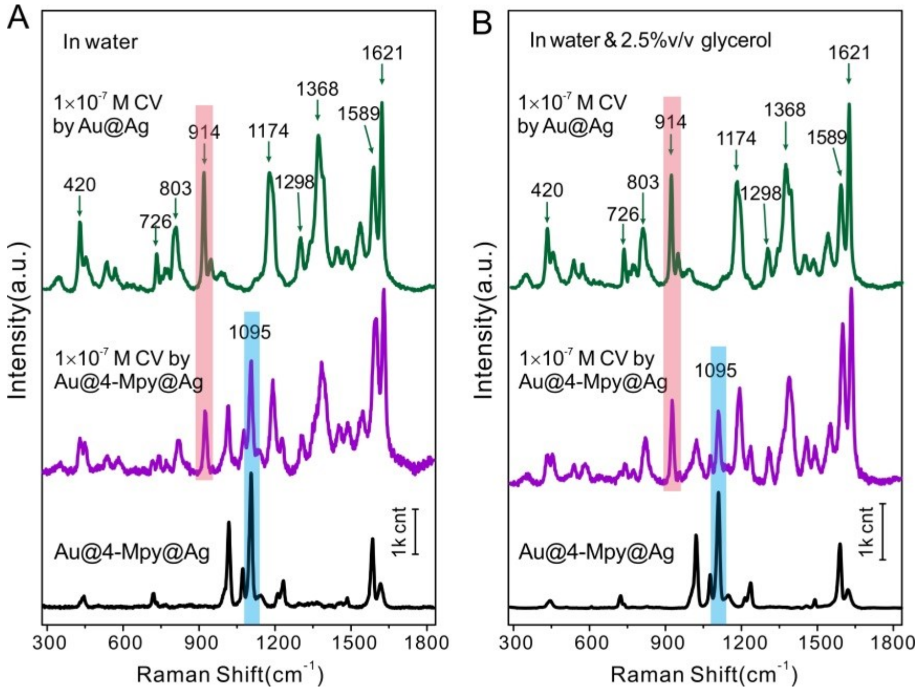

Fig.S9 A) In water-dispersed drying film system: SERS spectra of CV based Au@AgNPs, Au@4-Mpy@AgNPs and typical Raman spectra of Au@4-Mpy@AgNPs, respectively. B) In the glycerol-assisted liquid film protection system: SERS spectra of CV based Au@AgNPs, Au@4-Mpy@AgNPs and typical Raman spectra of Au@4-Mpy@AgNPs, respectively. The corresponding structural characterization of Au@AgNPs can be seen in Figure S6. The primary vibrations of CV are confirmed according to the literatures.[10-13]

Section 9: SEM and TEM characterization of Au@AgNPs.

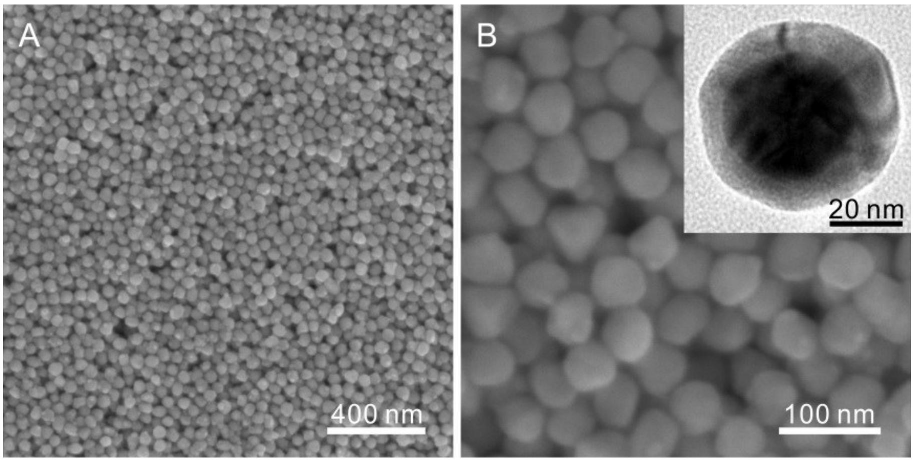

Fig.S10 Structural characterization of Au@AgNPs for comparative study: typical SEM images of A) and B) Au@AgNPs correspond to different magnifications; the inset of B) is the typical TEM image of Au@AgNPs.

References

1. Y. Wang, Z. Wei, Y. Zhang and Y. Chen, *Langmuir*, 2019, **35**, 15795-15804.
2. H. Liu, Z. Yang, L. Meng, y. sun, J. Wang, L. Yang, J. Liu and Z. Tian, *J. Am. Chem. Soc.*, 2014, **136**, 5332-5341.
3. Y. Sun, Z. Han, H. Liu, S. He, L. Yang and J. Liu, *Nanoscale*, 2015, **7**, 6619-6626.
4. E. C. L. Ru, E. Blackie, M. Meyer and P. G. Etchegoin, *J. Phys. Chem. C*, 2007, **111**, 13794-13803.
5. X. Tang, W. Cai, L. Yang and J. Liu, *Nanoscale*, 2013, **5**, 11193-11199.
6. W. Nam, X. Ren, S. A. S. Tali, P. Ghassemi, I. Kim, M. Agah and W. Zhou, *Nano Lett.*, 2019, **19**, 7273-7281.
7. H. Guo, L. Ding, T. Zhang and Y. Mo, *J. Mol. Struct.*, 2013, **1035**, 231-235.
8. N. Wattanavichean, M. Gilby, R. J. Nichols and H. Arnolds, *Anal. Chem.*, 2019, **91**, 2644-2651.
9. L. Bi, Y. Wang, Y. Yang, Y. Li, S. Mo, Q. Zheng and L. Chen, *ACS Applied Materials & Interfaces*, 2018, **10**, 15381-15387.
10. M. Li, J.-Y. Wang, Q.-Q. Chen, L.-H. Lin, P. Radjenovic, H. Zhang, S.-Y. Luo, Z.-Q. Tian and J.-F. Li, *Anal. Chem.*, 2019, **91**, 15025-15031.
11. X. Tang, W. Cai, L. Yang and J. Liu, *Nanoscale*, 2014, **6**, 8612-8616.
12. S. L. Kleinman, E. Ringe, N. Valley, K. L. Wustholz, E. Phillips, K. A. Scheidt, G. C. Schatz and R. P. Van Duyne, *J. Am. Chem. Soc.*, 2011, **133**, 4115-4122.
13. W. Meng, F. Hu, L. Zhang, X. Jiang, L. Lu and X. Wang, *J. Mol. Struct.*, 2013, **1035**, 326-331.